Submitted for publication in
Catalysis Communications (2009)

Deep oxidation of methane on particles derived from YSZ-supported Pd-Pt-(O) coatings synthesized by pulsed filtered cathodic arc.

D. Horwat[a,b*], J.L. Endrino[b,c], A. Boreave[d], R. Karoum[d], J.F. Pierson[a], S. Weber[e], A. Anders[b], Ph. Vernoux[d].

a Institut Jean Lamour, Département CP2S, Ecole des Mines, CS14234 Parc de Saurupt, F-54042, Nancy cedex, France
b Plasma Applications Group, Lawrence Berkeley National Laboratory, 1 Cyclotron Road, Berkeley, CA 94720, USA
c Instituto de Ciencias de Materiales de Madrid, Consejo Superior de Investigaciones Cientıficas, Campus de Cantoblanco, E-28049 Madrid, Spain
d Université Lyon 1, CNRS, UMR 5256, IRCELYON, Institut de recherches sur la catalyse et l'environnement de Lyon, 2 avenue Albert Einstein, F-69626 Villeurbanne, France
e Institut Jean Lamour, CC-MEM, Ecole des Mines, CS14234 Parc de Saurupt, F-54042 Nancy cedex, France

* Corresponding author. Tel.: +33 3 83 58 42 52.
E-mail address: david.horwat@mines.inpl-nancy.fr.

The work at Berkeley Lab was supported by the U.S. Department of Energy under Contract No. DE-AC02-05CH11231.

Deep oxidation of methane on particles derived from YSZ-supported Pd-Pt-(O) coatings synthesized by pulsed filtered cathodic arc.

D. Horwat[a,b*], J.L. Endrino[b,c], A. Boreave[d], R. Karoum[d], J.F. Pierson[a], S. Weber[e], A. Anders[b], Ph. Vernoux[d].

[a] Institut Jean Lamour, Département CP2S, Ecole des Mines, CS14234 Parc de Saurupt, F-54042 Nancy cedex, France
[b] Plasma Applications Group, Lawrence Berkeley National Laboratory, 1 Cyclotron Road, Berkeley, CA 94720, USA
[c] Instituto de Ciencias de Materiales de Madrid, Consejo Superior de Investigaciones Cientıficas, Campus de Cantoblanco, E-28049 Madrid, Spain
[d] Université Lyon 1, CNRS, UMR 5256, IRCELYON, Institut de recherches sur la catalyse et l'environnement de Lyon, 2 avenue Albert Einstein, F-69626 Villeurbanne, France
[e] Institut Jean Lamour, CC-MEM, Ecole des Mines, CS14234 Parc de Saurupt, F-54042 Nancy cedex, France

* Corresponding author. Tel.: +33 3 83 58 42 52.
E-mail address: david.horwat@mines.inpl-nancy.fr.

Abstract

Methane conversion tests were performed on Pd, PdO_y, $Pd_{0.6}Pt_{0.4}O_y$ and $Pd_{0.4}Pt_{0.6}O_y$ thin films deposited on yttria stabilized zirconia (YSZ) substrates. Pt containing films exhibited poor activity and high reducibility. As-deposited Pd and PdO_y films showed good activity and transformed, during the cycling process, to particles dispersed on the YSZ substrates. The higher reaction rate of initially PdO_y films was explained by a better dispersion of the catalyst. A drop of the reaction rate was observed when the temperature exceeded 735°C and 725°C for initially Pd and PdO_y, respectively, which can be associated with the high-temperature reduction of PdO into Pd.

1. Introduction

Improving the efficiency for the catalytic combustion of methane (CH_4) represents a challenge for the reduction of working temperature of CH_4 combustion turbines. Palladium catalysts have been shown to belong to the most effective catalysts for methane combustion (e.g. [1–6]) and to be more active than other transition metals for this reaction [5,7,8]. While bulk PdO is claimed to be inactive, a thin layer of PdO on metallic Pd is proposed to be the active form of palladium [8-10]. It was suggested that CH_4 combustion occurs via the Mars–van Krevelen mechanism where O_2 is assumed to oxidize the palladium surface, the formed surface oxide being reduced by CH_4 [4]. A bifunctional mechanism for methane oxidation over Pd/ZrO_2 catalysts has already been suggested, where metallic Pd particles dissociatively chemisorb methane producing adsorbed H and CH_X species [8,10]. Reoxidation rapidly converts the metal back to the oxide. The predominance of either metallic palladium-supported PdO or a Pd/PdO_y mixture for active oxidation of methane is still highly controversial. For Al_2O_3 support, the incorporation of Pt in Pd has been reported to improve and stabilize the catalytic oxidation of methane via Pd-Pt interaction (e.g. [12, 13]). On the contrary, Persson *et al.* observed superior conversion efficiency for Pd than Pd-Pt equimolar mixture, the latter presenting higher long term stability [14].

Pulsed Filtered Cathodic Vacuum Arc (PFCVA) can be successfully employed to deposit various chemical systems such as diamond like carbon (DLC), metal doped DLC [15, 16] and metal oxide [17, 18] films. The high reactivity of the evaporated species associated with the technique and the use of a dual cathode deposition system (DC-PFCVA) is expected to lead to the successful synthesis of binary and ternary noble metal oxide films. In the present study, yttria stabilized zirconia (YSZ) supported Pd-based catalysts were considered due to the applicability of YSZ

supports to solid oxide fuel cells and car engine exhausts where electrochemical promotion of catalysis start being considered [19, 20]. This study presents DC-PFCVA as a suitable technique to synthesize various metallic or oxide thin films for catalytic reactions, and explores the thermal evolution of the catalytic activity for YSZ-supported metallic Pd, Pd oxides and Pd_XPt_{1-X} oxides.

2. Experimental

2.1. Sample preparation

Metallic Pd, Pd oxide and Pd_XPt_{1-X} oxide films were prepared on YSZ pellets (14 mm in diameter, 1 mm thick). The system contains a dual-cathode “triggerless” mini-gun [21], which was designed to operate in pulsed mode. The two cathodes incorporated in the source were pure palladium and platinum. The pulsed operation of these cathodes was controlled using a custom National Instruments' LabView™ software. Once the computer has sent a signal to the arc power supply, an arc discharge pulse on a selected cathode is triggered simply by application of a high open circuit voltage (of about 600 V). The pulsed arc current employed was about 700 A with a pulse duration of about 1 ms. A pulse repetition rate of four pulses per second was employed for all films. The two mixed $Pd_{1-X}Pt_XO_Y$ films were deposited by alternating one platinum pulse and one palladium pulse for the higher Pt-containing $Pd_{1-X}Pt_XO_Y$ film, and one platinum pulse for every two palladium pulses for the lower Pt-containing $Pd_{1-X}Pt_XO_Y$ film. The plasma stream produced by the mini arc source was injected into a 90-degree filter to remove most of the macroparticles, which were formed during the cathodic arc evaporation process [22]. After exiting the

90-degree filter, the plasma stream travelled through a magnetic multipole homogenizer with 16.7 cm inner diameter in order to improve the film uniformity [22]. The substrate holder was grounded and rotated at a rate of 2 revolutions per minute during the deposition. The distance between the exit of the filter to the homogenizer was about 3 cm, and the distance from the magnetic homogenizer to the substrate was about 2 cm. The vacuum base pressure was typically in the 10^{-4} Pa range, the process pressure was set at approximately 2.13 Pa (16 mTorr). For the deposition of the pure palladium film, pure Ar was used as process gas while for the deposition of the oxide films pure oxygen was introduced to the chamber at 16 standard cubic centimeters per minute. The films were deposited at the same time on cubic YSZ pellets and silicon wafer pieces.

2.2. Sample characterization

The structural characteristics of the films were probed by grazing incidence X-ray diffraction (GIXRD) at an incident angle of 2° with respect to the substrate surface. The experiments were done with a Co-Kα source (wavelength of 0.178897 nm) using an INEL diffractometer. The film composition was measured by secondary neutral mass spectrometry (SNMS) with an 8 keV Ar^+ primary beam. The apparatus is a SimsLab-VG. The typical currents on the samples were in the range 300-500 nA and the sputtered atoms were post-ionised by the electrons emitted from a filament for the mass spectrometry analysis. The quantification procedure of the relative Pd and Pt content and the estimate of the oxygen content of as-grown films included, first, a calibration of the SNMS measurements using thick crystalline Pt_2O and PdO sputtered reference films, as well as SNMS measurements of a thick $Pd_{0.85}Pt_{0.15}O_y$

film whose metals stoichiometry was previously determined by energy dispersive spectroscopy (EDS). The compositions of thin catalyst films where then deduced from the integration of the SNMS profile corrected using the calibration. The surface of the Pd-based catalysts was observed by scanning electron microscopy (SEM, XL30S FEG Philips). Thickness measurements were carried out with a Dektak IIA profilometer on films deposited on flat silicon substrates.

Catalytic measurements were performed at atmospheric pressure in a specific quartz reactor described in a previous study [23, 24]. The catalysts were placed on sintered quartz, 18 mm in diameter. The reactive mixture passed through the porous disk from below and then licked the catalyst surface. A K-type thermocouple was located close to the catalytic surface. The reaction gases were mixtures of CH_4 (Air Liquide, 5% CH_4 in He) and O_2 (Air Liquide 5% O_2 in He). The gas composition was controlled by mass flow controllers (Brooks, with accuracies better than 1%). In the following, the gas composition will be expressed in ppm or %. The reactive mixture (RM) is containing CH_4/O_2: 5100 ppm/4%. The overall gas flow rate was kept with He constant at 72 mL min^{-1} (+/- 2 mL min^{-1}). To study the catalytic performance and the thermal ageing, three cycles were performed between 250°C and 800°C at a ramp of 10°C min^{-1} with a plateau of two hours at 800°C for each sample. The comparisons between catalytic surfaces of Pd, PdO, and $Pd_xPt_{1-x}O_y$ were performed during cycling. The reactants and products were analysed by an IPC400TM INFICON quadrupole mass spectrometer. Signals at m/e = 15, 18, 28, 32, 44 amu corresponding to CH_3^+, H_2O^+, N_2^+ or CO^+, O_2^+ and CO_2^+ ions, respectively, were recorded. The conversion of methane was defined as the percentage of methane

feed converted into CO_2. Carbon dioxide was the only oxidation product detected. The catalytic rate was calculated in reference to the palladium loading.

3. Results and discussions

Some characteristics concerning catalytic coatings are reported in Table. 1. The as-deposited Pd films were found to be nanocrystalline with an average grain size of about 10 nm while all the oxide films were amorphous. SEM examination of the samples revealed a complete coverage of the YSZ surface by the deposited materials with a dense morphology. While palladium oxide, PdO, and platinum dioxide, PtO_2, are stable in air at low temperatures, they start reducing in air at around 750°C [7] and 450°C [25], respectively. The estimated oxygen content in the as-deposited films (*y*) decreases with the incorporation of Pt. The methane conversion curves of the deposited films upon heating after a first RT-800°C-RT (RT: room temperature) thermal cycle are displayed on Fig. 1a. The Pd, PdO_y coatings promote methane deep oxidation upon heating below 770°C whereas the promotion by the $Pd_{0.6}Pt_{0.4}O_y$ film stops at roughly 750°C. The highest conversions occurred for as-deposited Pd and PdO_y films. Very low catalytic activity is observed on $Pd_{0.4}Pt_{0.6}O_y$ film. The present results are in accordance with the detrimental effect of Pt incorporation into $Pd_{1-x}Pt_x$ for $x \geq 0.33$ reported by Persson *et al.* for the same reaction [14].

For a better comparison of the different catalysts, the reaction rate has been calculated in reference to the palladium loading (Fig.1 b). The representation highlights a superior catalytic activity of as-deposited palladium oxide films compared

to metallic palladium. The behavior of $Pd_{0.6}Pt_{0.4}O_y$ is characterized by lower activity between 580°C and 680°C. This might be related to the onset of the reduction of oxidized platinum. In this context, it is worth noting that Seriani *et al.* calculated a higher efficiency of platinum oxide (Pt_3O_4) than Pt for CH_4 cracking [26]. We believe that the strong platinum reducibility explains the improved reducibility of the compound, leading to a reaction rate drop at 680°C for $Pd_{0.6}Pt_{0.4}O_y$ and of the negligible activity for $Pd_{0.4}Pt_{0.6}O_y$.

The thermal cycling behavior of the as-deposited Pd and PdO_y films is shown in Fig. 2. Starting from metallic palladium, the onset of the catalytic conversion is observed at 550°C upon the first heat up, whereas PdO_y is already active at 400°C. The reaction rate drops at 735°C and 725°C for initially Pd and PdO_y films, respectively. These temperatures cause the reduction of PdO into metallic Pd. They are higher than the 700°C reported in oxidizing mixtures by Furuya *et al.* for Pd nanoparticles on YSZ [27], and the 715°C reported by Roche *et al.* for 52-nm thick Pd thin films sputter-deposited on YSZ [28]. Cooling down the samples from 800°C, surface re-oxidation occurs, thereby restarting the conversion the hydrocarbons. However, the reoxidation of the surface occurs at a lower temperature than the reduction upon heating. Both materials exhibit an activity hysteresis of about 100°C. The phenomenon is qualitatively consistent with the original observation by Farrauto *et al.* for Al_2O_3-supported Pd [7]. The thermal cycling of PdO_y did not give any evidence for strong differences between the cycles. In the case of Pd, the first heating is associated to a lower activity. This indicates a strong structural or/and chemical evolution of the Pd film during the first heating. From the previous discussion, the reducibility of the compounds drives the thermal evolution of the catalytic activity. Palladium was the only crystalline as-deposited film. The GIXRD

signature of the different samples after the third cycle is represented on Fig.3. These investigations interestingly highlight that the final structural state is very sensitive to the initial composition:

- The only phase detected for Pt-containing films is metallic (no Pt oxide).
- The as-deposited Pd film transformed into a biphased alloy consisting of Pd and PdO.
- The as-deposited PdO_y film converted into crystalline PdO. The reddish colour characteristic of PdO could be observed only for that sample.

Therefore, the hypothesis of the higher reducibility of Pt-containing films is confirmed. The SEM observation of both initially Pd and PdO_y films shows an important evolution of the morphology towards clusters of particles dispersed at the surface of the zirconia substrate (Fig. 4). PdO_y evolved in jagged clusters of few particles with a characteristic size of the particles close to 100 nm. The clusters derived from the Pd film are bigger and more spherical in shape. Significant coalescence occurred between the particles. The differences in shapes and sizes are linked to strong differences in the surface to volume ratio. Using a spherical approximation for the particle shape, the dispersion of the catalyst was estimated to 6 and 16 % for initially Pd and PdO_y films respectively. Assuming a surface oxidation for both compounds within the thermal domain of active heterogeneous catalysis, the latter parameter obviously explains the discrepancy between the maximal activities of the two compounds.

Conclusions

Methane conversion tests were performed on Pd, PdO_y, $Pd_{0.6}Pt_{0.4}O_y$ and $Pd_{0.4}Pt_{0.6}O_y$ thin films deposited by Dual Cathode Filtered Cathodic Vacuum Arc on YSZ substrates. The catalytic activity curves over thermal cycling were discussed in terms of the reducibility of the deposited compounds. The film with the highest Pt content exhibited poor activity and $Pd_{0.6}Pt_{0.4}O_y$ showed limited activity and high reducibility. In contrast, during the cycling process, the as-deposited Pd and PdO_y films showed good activity despite the transformation to clusters of particles dispersed on the YSZ substrates. The higher reaction rate of the initially PdO_y films was explained by a better dispersion of the catalyst. The drop in the reaction rate, associated with the reduction of PdO into Pd at high temperature, was measured at 735°C and 725°C for the initially Pd and PdO_y films, respectively. After three thermal cycles up to 800°C, it was not possible to detect either Pd or Pt oxides in the Pt containing films. As-deposited Pd evolved to a Pd/PdO mixtures, only crystalline PdO was detected for initially PdO_y amorphous films.

Acknowledgments

Work at Berkeley Lab was supported by the U.S. Department of Energy under Contract No. DE-AC02-05CH11231.

References

[1] F. H. Ribeiro, M. Chow and R. A. DallaBetta, J. Catal. 146 (1994) 537.

[2] C.A.Müller, M. Maciejewski, R. A. Koeppel, R. Tschan and A. Baiker, J. Phys. Chem. 100 (1996) 20 006.

[3] K. Fujimoto, F. H. Ribeiro, M. Avalos-Borja and E. Iglesia, J. Catal. 179 (1998) 431.

[4] R. A. DallaBeta and T. Rostrup-Nielsen, Catal. Today 47 (1999) 369.

[5] G. Centi, J. Mol. Catal. A 173 (2001) 287.

[6] P. Gelin and M. Primet, Appl. Catal. B 39 (2002) 1

[7] R. J. Farrauto, M. C. Hobson, T. Kennelly and E. M. Waterman, Appl. Catal. A 81 (1992) 227

[8] J.N. Carstens, S.C. Su and A.T. Bell, J. Catal. 176 (1998) 136

[9] R. Burch and F. J. Urbano, Appl. Catal. A 124 (1995) 121

[10] S.C. Su, J.N. Carstens and A. T. Bell, J. Catal. 176 (1998) 125

[11] S. Yang, A. Maroto-Valientea, M. Benito-Gonzaleza, I. Rodriguez-Ramosa and A. Guerrero-Ruiz, Appl. Catal. B 28 (2000) 223

[12] G. Lapisardi, L. Urfels, P. Gelin, M. Primet, A. Kaddouri, E. Garbowski, S. Toppi, E. Tena, Catal. Today 117 (2006) 564

[13] H. Yamamoto, H. Uchida, Catal. Today 45 (1998) 147

[14] K. Persson, A. Erssona, K. Janssonb, N. Iverlund, S. Järås, J.Catal. 231 (2005) 139

[15] J.L. Endrino, R. Escobar Galindo, H.-S. Zhang, M. Allen, R. Gago, A. Espinosa, A. Anders, Surf. Coat. Technol. 202 (2008) 3675

[16] J.L. Endrino, D. Horwat, R. Gago, J. Andersson, Y.S. Liu, J. Guo, A. Anders, Sol. Stat. Sci, In Press, corrected proofs, DOI: 10.1016/j.solidstatesciences.2008.08.007

[17] S. Anders, A. Anders, M. Rubin, Z. Wang, S. Raoux, F. Kong, I.G. Brown, Surf. Coat. Technol. 76-77 (1995) 167

[18] R.A. MacGill, S. Anders, A. Anders, R.A. Castro, M. R. Dickinson, K.M. Yu, I.G. Brown, Surf. Coat. Technol. 78 (1996) 168

[19] C.G. Vayenas, S. Bebelis, C. Pliangos, S. Brosda, D. Tsiplakides (2001) Electrochemical Activation of Catalysis: Promotion, Electrochemical Promotion Metal-Support Interactions. Kluwer Academic/Plenum, New York

[20] X. Li, F. Gaillard, P. Vernoux, Topics in Catalysis 44 (2007) 391

[21] A. Anders, N. Pasaja, and S. Sansongsiri, Rev. Sci. Instrum., 78 (2007) 063901

[22] A. Anders, Cathodic Arcs: From Fractal Spots to Energetic Condensation. New York: Springer, 2008

[23] P. Vernoux, F. Gaillard, L. Bultel, E. Siebert, M. Primet, J. Catal. 208 (2002) 412

[24] F. Gaillard, X. Li, M. Uray, P. Vernoux, Catal. Letters 96 (2004)177

[25] K.L. Saenger, C. Cabral Jr. C. Lavoie, S.M. Rossnagel, J. Appl. Phys. 86 (1999) 6084

[26] N. Seriani, W. Pompe, L. Colombi Ciacchi, J. Phys. Chem. B (2006) 14860

[27] T. Furuya, K. Sasaki, Y. Hanakata, T. Ohhashi, M. Yamada, T. Tsuchiya, Y. Furuse, Catal. Today 26 (1995) 345

[28] V. Roche, R. Karoum, A. Billard, R. Revel, P. Vernoux, J. Appl. Electrochem. 38 (2008) 1111

Table caption

Table 1: Some characteristics of the deposited catalysts. * As-deposited.

Figure captions

Figure 1: Methane conversion a), methane reaction rate in reference to the Pd load b) over the deposited compounds during the second heat up from 250°C to 800°C.

Figure 2: Evolution of the methane reaction rate during thermal cycling.

Figure 3: X-ray diffraction patterns of the deposited compounds after thermal cycling.

Figure 4: PdO particles derived from thermally cycled PdO_y films deposited films a), mixed PdO + Pd particle clusters derived from thermally cycled Pd films deposited films b).

Figure 1a

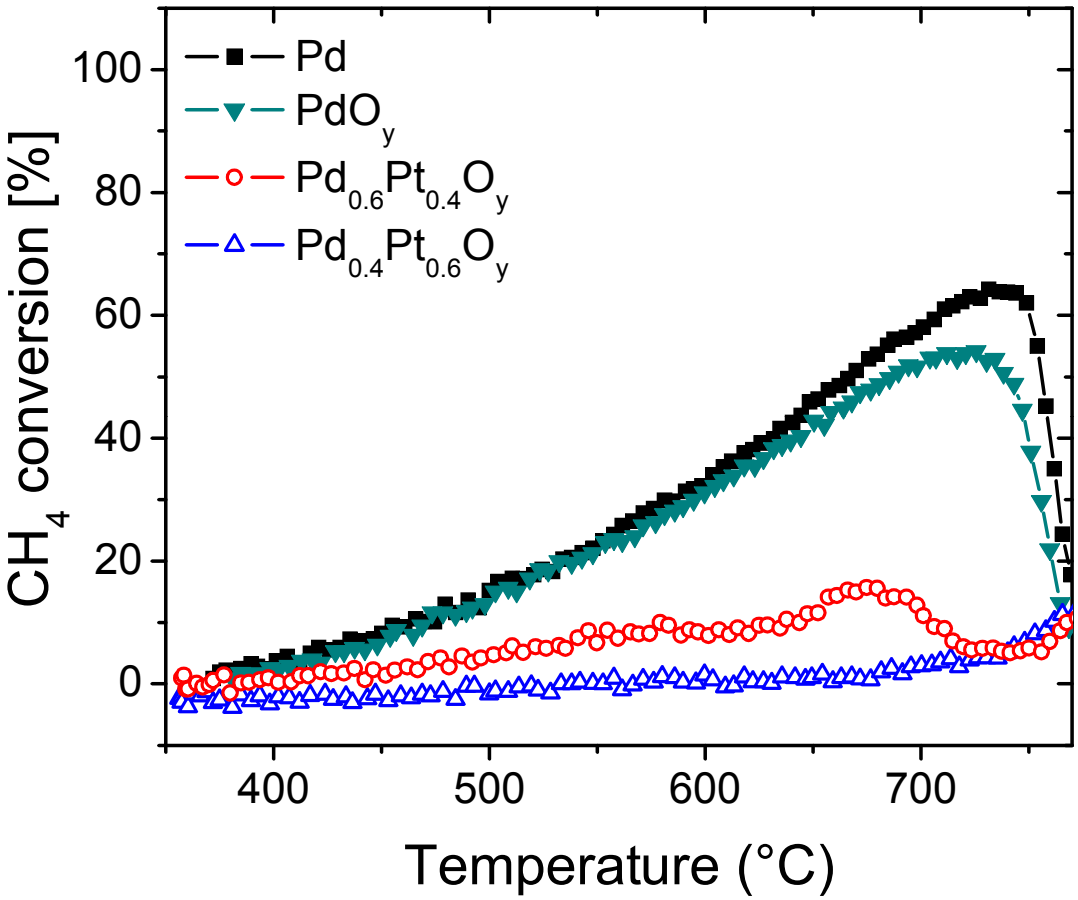
Pd
PdO$_y$
Pd$_{0.6}$Pt$_{0.4}$O$_y$
Pd$_{0.4}$Pt$_{0.6}$O$_y$
CH$_4$ conversion [%]
0
20
40
60
80
100
400
500
600
700
Temperature (°C)

Figure 1b

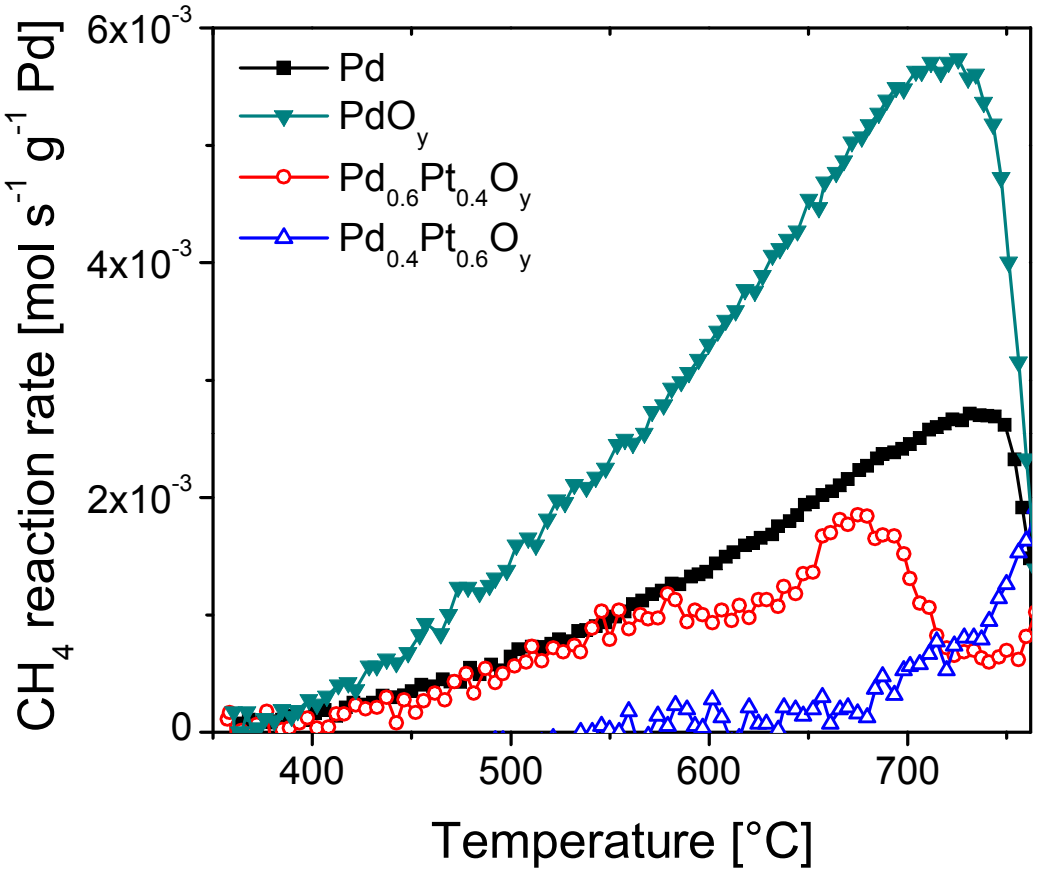
6x10-3
4x10-3
2x10-3
0
CH4 reaction rate [mol s-1 g-1 Pd]
Pd
PdOy
Pd0.6Pt0.4Oy
Pd0.4Pt0.6Oy
400
500
600
700
Temperature [°C]

Figure 2

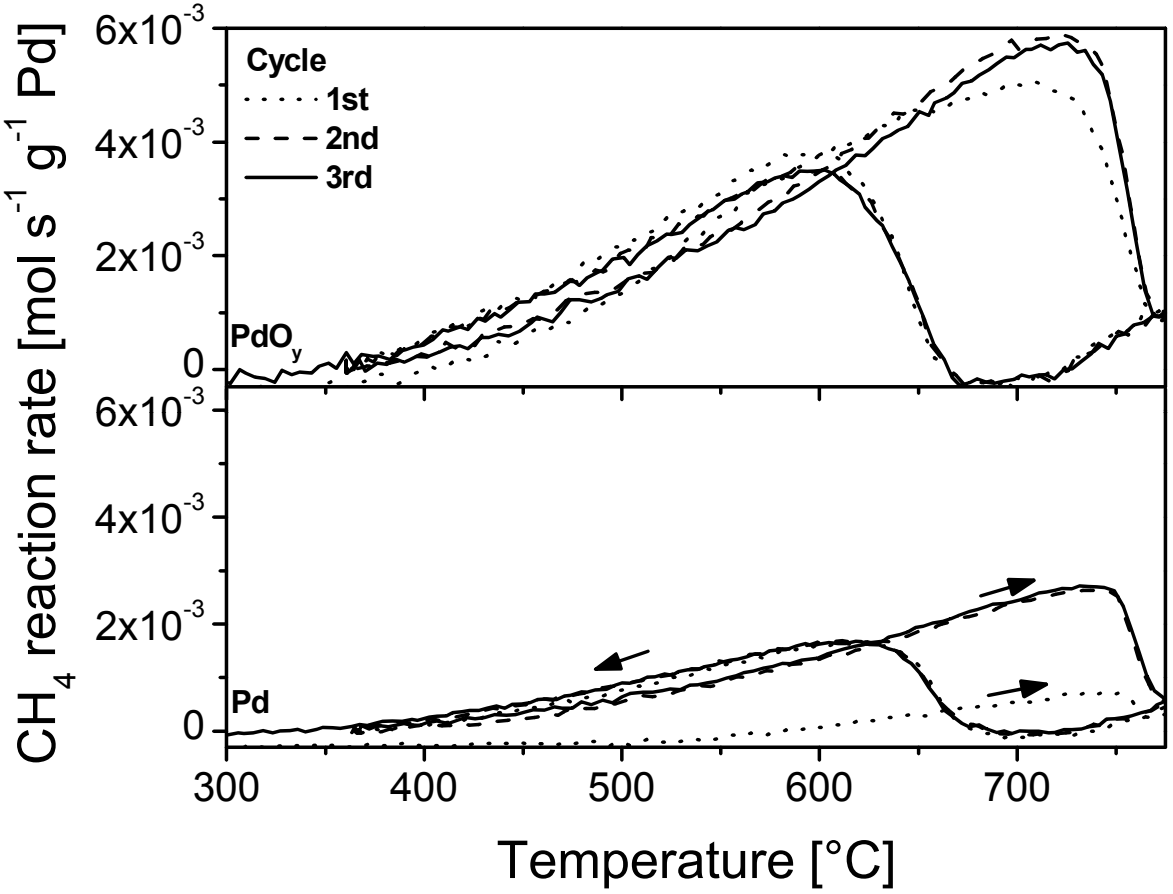
Cycle
1st
2nd
3rd
PdO$_y$
Pd
6x10^{-3}
4x10^{-3}
2x10^{-3}
0
300
400
500
600
700
CH$_4$ reaction rate [mol s^{-1} g^{-1} Pd]
Temperature [°C]

Figure 3

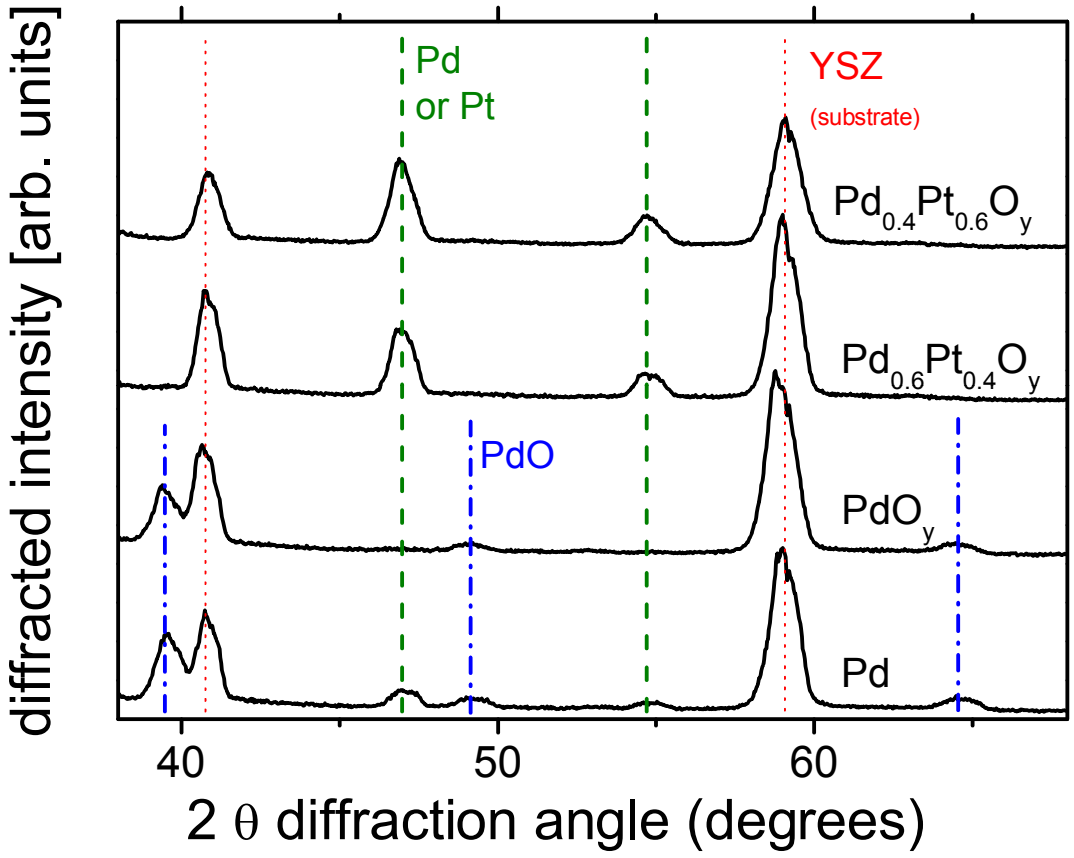
diffracted intensity [arb. units]
Pd
or Pt
YSZ
(substrate)
Pd0.4Pt0.6Oy
Pd0.6Pt0.4Oy
PdO
PdOy
Pd
40
50
60
2 θ diffraction angle (degrees)

Figure 4

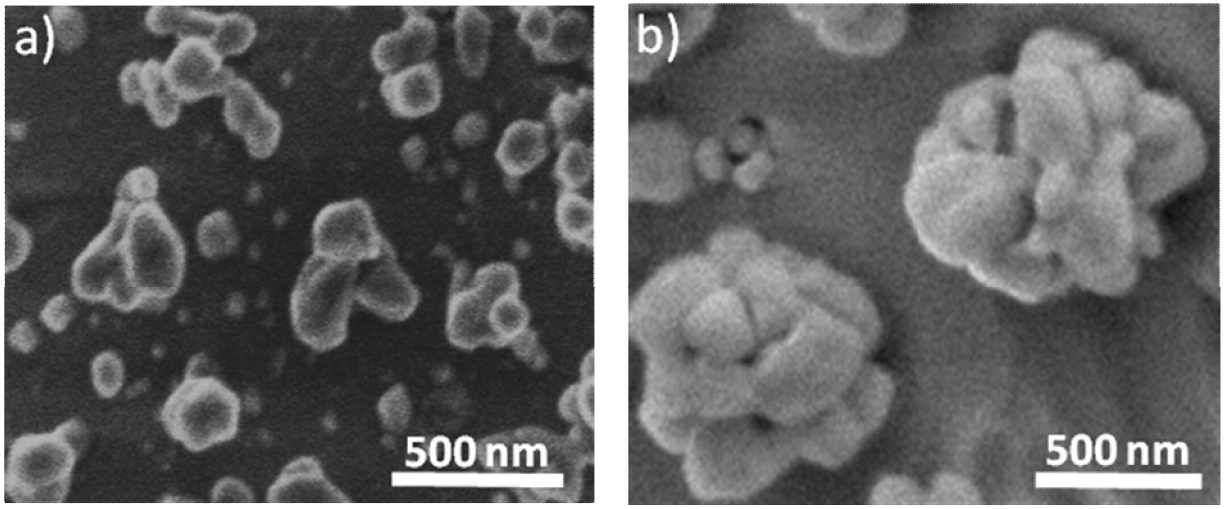

Table 1

Composition	Initial structure	Thickness (nm)	Oxygen/Metal (y) *	Pd loading (μg)	Final structure (3 cycles)	Maximal catalytic rate (mmol CH_4 s^{-1} g^{-1} Pd)
Pd	nano-crystalline (~10 nm)	45	/	83	Pd + PdO	2.57
PdO_y	amorphous	34	0.96	40	PdO	5.9
$Pd_{0.6}Pt_{0.4}O_y$	amorphous	37	0.74	36	Metal	1.85
$Pd_{0.4}Pt_{0.6}O_y$	amorphous	35	0.63	23	Metal	/